Scientific Research Publishing

Journal of Applied Mathematics and Physics, 2026, 14(6), 2238-2249
https://www.scirp.org/journal/jamp
ISSN Online: 2327-4379
ISSN Print: 2327-4352

The Angular Distribution Effect of Electron-Positron Pair Production

Yara Owaidh Althurwi, Sadah Abdullah Alkhateeb, Nada Ahmed Almuallem

Department of Mathematics and Statistics, Faculty of Science, University of Jeddah, Jeddah, Saudi Arabia
Email: yara5524@gmail.com

How to cite this paper: Althurwi, Y.O., Alkhateeb, S.A. and Almuallem, N.A. (2026) The Angular Distribution Effect of Electron-Positron Pair Production. *Journal of Applied Mathematics and Physics*, **14**, 2238-2249.
https://doi.org/10.4236/jamp.2026.146109

Received: April 20, 2026
Accepted: June 15, 2026
Published: June 18, 2026

Copyright © 2026 by author(s) and Scientific Research Publishing Inc.
This work is licensed under the Creative Commons Attribution International License (CC BY 4.0).
http://creativecommons.org/licenses/by/4.0/

Open Access

Abstract

This study investigates the theoretical aspects of electron-positron pair production in light and medium nuclei using quantum electrodynamics (QED) formulations. By employing computational tools such as Mathematica, we analyze the dependence of pair generation rates on nuclear charge, angular distribution, and interaction cross-sections. Special attention is given to the comparative roles of electric and magnetic multipole contributions in shaping production probability. Graphical results are presented to illustrate how the pair production threshold and efficiency vary with both the incident photon angle and nuclear mass. Our findings suggest that lighter nuclei exhibit enhanced pair production efficiency, while higher photon energies amplify the influence of multipole effects. These insights provide useful implications not only for fundamental nuclear physics but also for applied fields such as medical imaging, where precise control of electron-positron pair dynamics is central to technologies like positron emission tomography (PET).

Keywords

Pair Production, Bethe-Heitler Equation, Angular Distribution, Cross Section

1. Introduction

The theory of quantum mechanics that Schrödinger and Heisenberg proposed works only for nonrelativistic phenomena. This theory, which is called nonrelativistic quantum mechanics, was immensely successful in explaining a wide range of such phenomena. Combining the theory of special relativity with quantum mechanics, Dirac succeeded (1928) [1] in extending quantum mechanics to the realm of relativistic phenomena. The new theory, called relativistic quantum mechanics, predicted the existence of a new particle, the positron. This particle, defined as the

antiparticle of the electron, was predicted to have the same mass as the electron and an equal but opposite (positive) charge [2].

Four years after its prediction by Dirac's relativistic quantum mechanics, the positron was discovered by Anderson in 1932 [2] while studying the trails left by cosmic rays in a cloud chamber. When high-frequency electromagnetic radiation passes through a foil, individual photons of this radiation disappear by producing a pair of particles consisting of an electron, e^-, and a positron, e^+:

$$\text{photon} \to e^- + e^+ .$$

This process is called pair production [3].

At the beginning, pair production was investigated in terms of constant electric fields only [4]. Due to the arising of new tools applicable for studying matter creation, the focus shifted to time-dependent electric fields still neglecting magnetic fields entirely [5] [6]. Research of pair production for arbitrarily, complicated time-dependent electric fields [7]-[12] as well as first calculations for space-dependent background fields shed further light of our understanding of the formation of matter [13]-[18]. Additionally, parallel as well as collinear electric and magnetic fields have been considered [19]-[21].

It is important to distinguish between different pair production mechanisms. In this study, we focus exclusively on the Bethe-Heitler process, where pair production occurs in the electromagnetic field of a nucleus. This mechanism differs fundamentally from Schwinger-type pair production, which arises in strong external fields and vacuum conditions. The present work does not consider vacuum pair production effects but rather concentrates on photon-nucleus interactions.

The first theoretical studies on pair production undertaken in the 1930's [22]-[25]. Hubbell [26] provides a historical overview of the $\left(e^-e^+\right)$ by photons from Dirac's prediction of the position in 1928 until 2006. The (DCS) results for $\left(e^-e^+\right)$-Hubbell and Seltzer [27] revealed photon-based Pair Production. There is still much scientific research on this topic, and in 2020, Sadah studied the effect of nuclear magnetic distribution on the photon production of longitudinally polarized lepton-pairs in the field of Na_{11}^{23} and Al_{13}^{27} nuclei [28]. In 2022, Alkhateeb, S., Alshaery, A. and Aldosary, R. studied the Electron-positron pair production in Electro-Magnetic Field [29]. Finally, in 2025 Yara, Sadah and Nada studied the e^-e^+ pair production using high energy [30].

As it is of essential importance to understand what could happen when using PET [31], our goal for this thesis is to broaden the knowledge regarding electron-positron pair production. This topic is deeply connected with particle creation. Besides matter creation in the early universe, particle creation as one key process in order to interpret astrophysical measurements, for example Hawking radiation [32] or pair instability supernovas [33]. Nonetheless, particle production is not only restricted to astrophysics. Returning to the particular case of electron-positron pair production the advances in Laser technology provide us with novel possibilities. If particle production were feasible in a laboratory under controlled conditions, it would provide us with a powerful new tool to study high-energy pro-

cesses with unprecedented precision.

In our previous work [30], we studied electron-positron pair production at intermediate and high photon energies. We used aluminum (Al_{13}^{25}) and beryllium (Be_4^9) nuclei as targets to determine which energy ranges produce pairs most efficiently. By comparing these nuclei, we showed how nuclear mass and charge affect pair production and identified the optimal energy conditions.

In this paper, we focus on how the angle of incoming photons affects electron-positron pair production. We test different photon incidence angles with aluminum (Al_{13}^{25}) and beryllium (Be_4^9) nuclei. We also compare which nucleus responds more strongly to changes in angle. Additionally, the study examines the effect of the photon incidence angle on both the electric field and magnetic field contributions to the process. A comparative analysis is performed to determine which field plays a more dominant role and which nuclear target provides more favorable conditions for electron-positron pair production. The results of this work aim to identify the optimal incidence angles and nuclear targets that maximize the efficiency of electron-positron pair production.

2. Research Methodology

In this section, we discuss the interaction of a photon with Be_4^9 and Al_{13}^{25} nucleus produces pairs of e^-e^+. A schematic representation of the electron-positron pair production process in the electromagnetic field of a nucleus is shown in **Figure 1**. The e^-e^+ process produced by the interaction of the γ-photon field with the nuclei field (N) can be written as:

$$\gamma + N \rightarrow N + e^-e^+$$

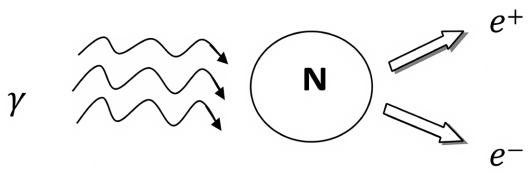

Figure 1. Simplified representation of a beam of high-energy photons colliding with a nucleus, resulting in the production of an electron-positron pair [29].

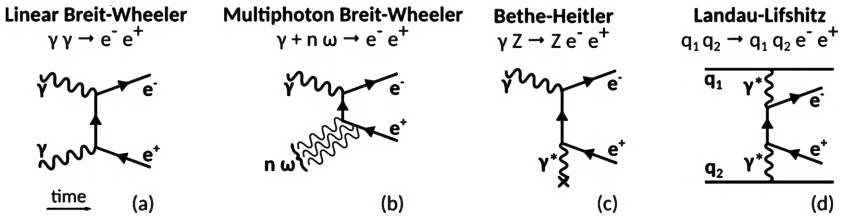

Figure 2. Examples of pair production. In (a) the collision of one high energy photon with several low energy photons by photon-photon collision processes. In (b) the collision of a real photon with an electric field interpreted in the theoretical framework of QED as a virtual photon (such as the Bethe-Heitler process when the electric field arises from atomic nuclei, (c)) or through the collision of two virtual photons in charged particle collisions (Landau-Lifshitz process for charges q_1 and q_2 in (d)) [34].

Different mechanisms of electron-positron pair production are illustrated in **Figure 2.** Also, the depiction of the Feynman diagrams for the issue of $e^{-}e^{+}$ pair production in the electromagnetic field of the nuclei has presented in the following diagram:

In this work, the Bethe-Heitler formalism is adopted within the framework of QED to provide a quantitative description of electron-positron pair production in the electromagnetic field of light nuclei. Particular attention is devoted to the dependence of the production mechanism on the incident photon energy, as well as to the role of photon scattering kinematics, including angular distributions associated with the interaction. In addition, the Bethe-Hitler equation for the electron-positron pair production process can be presented as follows:

$$\begin{aligned} d\sigma_{BH} = {} & \frac{Z^2\alpha^3}{(2\pi)^2}\frac{|p_-||p_+|dE_+}{\omega^3}\frac{d\Omega_- d\Omega_+}{|q|^4}\left[\frac{p_-^2\sin^2\theta}{(E_- - p_-\cos\theta_-)^2}\left(4E_+^2 - q^2\right)\right. \\ & - \frac{p_+^2\sin^2\theta_+}{(E_+ - p_+\cos\theta_+)^2}\left(4E_-^2 - q^2\right) + 2\omega^2\frac{p_+^2\sin^2\theta_+ + p_-^2\sin^2\theta}{(E_+ - p_+\cos\theta_+)(E_- - p_-\cos\theta_-)} \\ & \left. - \frac{2p_+p_-\sin\theta_+\sin\theta_-\cos\phi}{(E_+ - p_+\cos\theta_+)(E_- - p_-\cos\theta_-)}\left(2E_+^2 - 2E_-^2 - q^2\right)\right] \end{aligned} \quad (1)$$

This equation is the Bethe-Hitler equation for the electron-positron pair production process, and it can be written in an abbreviated form so that it is applicable using the following symbols:

$$d(\theta, Ze, \mu_1, Q, \Omega) = d\sigma_{oe}(\theta) + d\sigma_{om}(\theta) + d\sigma_{oq}(\theta) + d\sigma_{o\Omega}(\theta). \quad (2)$$

$$d\sigma_{oe}(\theta) = 8\pi\eta\phi_{oe}(\theta)d\Omega, \quad (3)$$

$$d\sigma_{om}(\theta) = 8\pi\eta\left(\frac{\mu_1}{Ze}\right)^2 a_\mu\phi_{om}(\theta)d\Omega, \quad (4)$$

$$d\sigma_{oq}(\theta) = 8\pi\eta\left(\frac{\Omega}{Ze}\right)^2 a_q\phi_{oq}(\theta)d\Omega, \quad (5)$$

$$d\sigma_{o\Omega}(\theta) = 8\pi\eta\left(\frac{\Omega}{Ze}\right)^2 a_\Omega\phi_{o\Omega}(\theta)d\Omega, \quad (6)$$

where

$$\eta = \left(\frac{Z^2\alpha^3}{4\pi^2}\right)\frac{p_+p_-dE_+}{\omega^3},\ \Delta_0 = (1-\cos\theta),$$

$$p_+ = \left|\overrightarrow{p_+}\right|,\ p_- = \left|\overrightarrow{p_-}\right|,$$

$\omega = E_+ + E_-$, ω is the energy of the colliding photon.

The Ze, μ_1, Q and Ω are electric charge $d\sigma_{oe}$, magnetic dipole $d\sigma_{om}$, electric quadrupole $d\sigma_{oq}$, magnetic octupole $d\sigma_{o\Omega}$, total electric dE and total magnetic dM moments of the target nucleus, respectively. The $\phi_{oe}(\theta)$, $\phi_{om}(\theta)$, $\phi_{oq}(\theta)$ and $\phi_{o\Omega}(\theta)$ in the case of high energy $E, E' \gg m_0c^2$. Also, we obtain the values $\phi_{oe}(\theta)$, $\phi_{om}(\theta)$, $\phi_{oq}(\theta)$ and $\phi_{o\Omega}(\theta)$ from research [29].

Where ε denotes the incident photon energy, ω represents the photon frequency, and θ is the scattering angle. The symbols $\theta_{\pm}$ refer to the emission angles of the electron and positron, respectively, while φ is the azimuthal angle. The differential cross-section components are defined as follows: $d\sigma_{oe}$ corresponds to the electric charge contribution, $d\sigma_{om}$ to the magnetic dipole, $d\sigma_{oq}$ to the electric quadrupole, and $d\sigma_{o\Omega}$ to the magnetic octupole contribution. The total electric and magnetic contributions are given by ($dE = d\sigma_{oe} + d\sigma_{oq}$) and ($dM = d\sigma_{om} + d\sigma_{o\Omega}$), respectively.

The high-energy approximation used in this work is valid since the incident photon energies ($\varepsilon \gg m_0c^2$) are significantly larger than the electron rest mass, which justifies the use of the Bethe-Heitler formalism [24].

In this work, the scattering angle θ is fixed for each calculation, while integration over other angular variables is implicitly included within the adopted Bethe-Heitler formalism.

The numerical inputs used in this study are based on previously reported nuclear parameters. For the Be_4^9 and Al_{13}^{25} nuclei, the nuclear charge Z and the corresponding electric and magnetic multipole moments were adopted from Ref. [30]. All calculations were performed using standard units, with photon energies expressed in MeV. The electron rest mass was taken as $m = 0.511$ MeV/c^2, and natural units ($\hbar = c = 1$) were used throughout the analysis. All numerical computations were carried out using Mathematica. The Bethe-Heitler differential cross-section expressions were evaluated for fixed photon energies ($\varepsilon = 500$, 700, 900 MeV) and scattering angles ($\theta = 100^\circ, 120^\circ, 140^\circ$). The relevant parameters were held constant while varying the photon energy and angle to construct a discrete energy-angle grid. The resulting values were used to compute and plot the differential cross sections for the electric and magnetic multipole contributions.

3. Results and Discussion

In this section, we will discuss the effect of different angles on the e^-e^+ pair production process, as well as the impact of nuclear mass on this process, we will also study the effect of the electric and magnetic fields on the e^-e^+ pair production process.

3.1. The Effect of Different Angels and Energies for Be_4^9 and Al_{13}^{25} Nucleus on the Electron-Positron Pair Production Process

From Equations (1)-(6), the parameters $d\sigma_{oe}$, $d\sigma_{om}$, $d\sigma_{oq}$ and $d\sigma_{o\Omega}$ represent the electric charge, magnetic dipole, electric quadrupole and magnetic octupole, respectively. Parameters dE and dM denote the total electric field and total magnetic field. Differential cross section for the electron-positron pair production using formulas for the angle distribution is obtained for the nuclei Be_4^9 and Al_{13}^{25} at different values of incident angles $\theta = (100^\circ, 120^\circ, 140^\circ)$ and the incident photon energies $\varepsilon = (500, 700, 900)$ MeV, where $m = 0.910940637872524 \times 10^{-27}$

mass of electron.

From Table 1, Table 2 and Figure 3, Figure 4, we can see that:

- The phenomenon of electron-positron pair production significantly enhances the understanding of particle interactions, particularly through its impact on differential cross-sections $d\sigma_{oe}$ and $d\sigma_{om}$. As photon energy diminishes and the angle of incidence varies, these cross-sections demonstrate a marked increase, highlighting the intricate relationships between energy and angular distribution in high-energy physics. Notably, this interaction reaches its peak effectiveness at approximately $\varepsilon = 500$ MeV and $\theta = 100^{\circ}$.
- The differential cross-section $d\sigma_{oq}$ increase for electron-positron pair production as the incident photon angle decreases and photon energy increases. The maximum value is observed at $\varepsilon = 900$ MeV and $\theta = 100^{\circ}$.
- The differential cross-section $d\sigma_{o\Omega}$ increase for electron-positron pair production as the incident photon angle and photon energy increase. The maximum value is observed at $\varepsilon = 900$ MeV and $\theta = 140^{\circ}$.

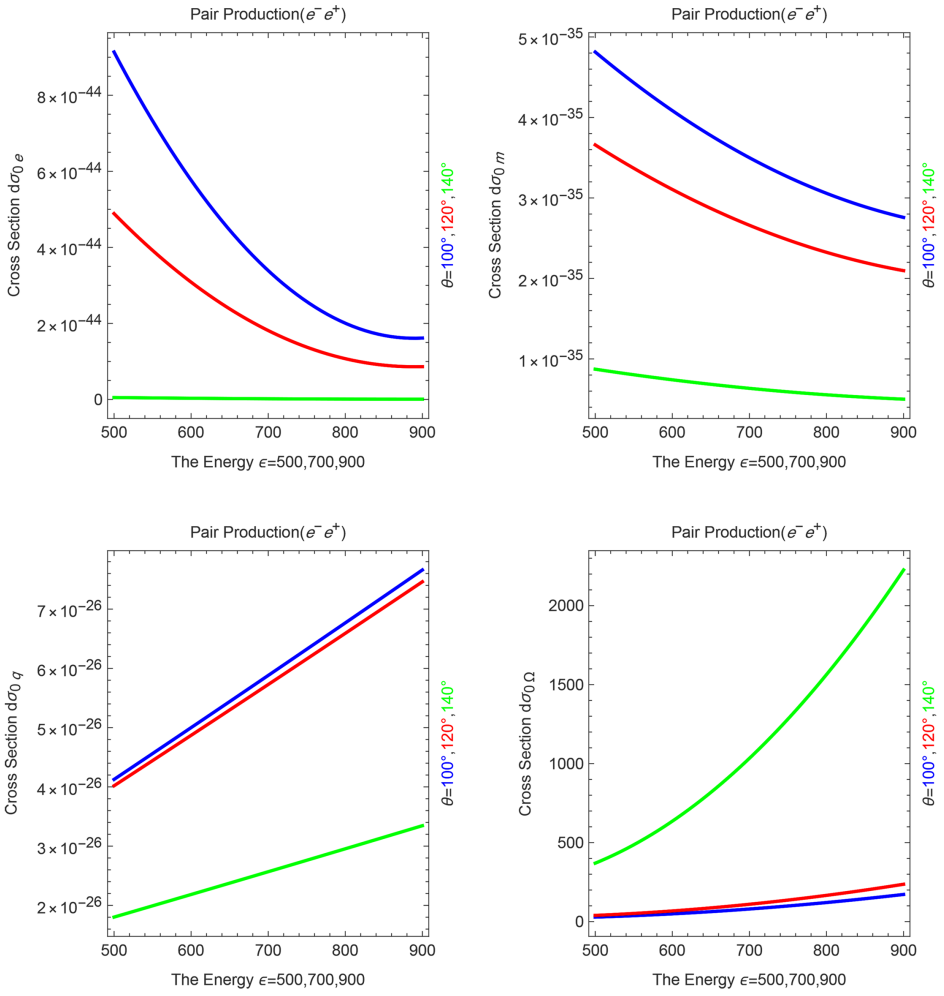

Figure 3. The DCS Electric Charge $d\sigma_{oe}$, Magnetic Dipole $d\sigma_{om}$, Electric Quadrupole $d\sigma_{oq}$ and Magnetic Octupole $d\sigma_{o\Omega}$ for the nuclei Be_4^9.

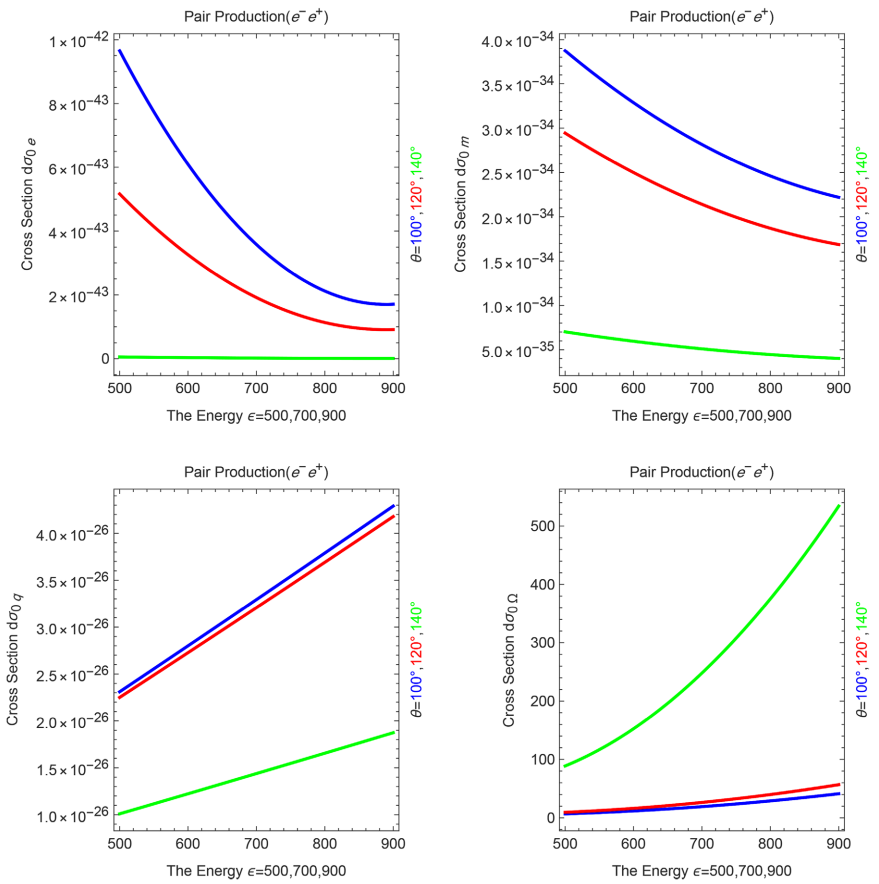

Figure 4. The DCS Electric Charge $d\sigma_{oe}$, Magnetic Dipole $d\sigma_{om}$, Electric Quadrupole $d\sigma_{oq}$ and Magnetic Octupole $d\sigma_{o\Omega}$ for the nuclei Al_{13}^{25}.

Table 1. DCS of the angle distribution for the Be_4^9 nuclei.

θ	ε	$d\sigma_{0e}$	$d\sigma_{0m}$	$d\sigma_{0q}$	$d\sigma_{0\Omega}$	dE	dM
100	500	9.13728×10^{-44}	4.81326×10^{-35}	4.12593×10^{-26}	28.5805	4.12593×10^{-26}	28.5805
100	700	3.38986×10^{-44}	3.49988×10^{-35}	5.88034×10^{-26}	79.8434	5.88034×10^{-26}	79.8434
100	900	1.61602×10^{-44}	2.75805×10^{-35}	7.66036×10^{-26}	171.948	7.66036×10^{-26}	171.948
120	500	4.88851×10^{-44}	3.65909×10^{-35}	4.01854×10^{-26}	39.3159	4.01854×10^{-26}	39.3159
120	700	1.81359×10^{-44}	2.66066×10^{-35}	5.72731×10^{-26}	109.84	5.72731×10^{-26}	109.84
120	900	8.64574×10^{-45}	2.09672×10^{-35}	7.46102×10^{-26}	236.558	7.46102×10^{-26}	236.558
140	500	5.23947×10^{-46}	8.72422×10^{-36}	1.80245×10^{-26}	369.942	1.80245×10^{-26}	369.942
140	700	1.94355×10^{-46}	6.34404×10^{-36}	2.56824×10^{-26}	1033.58	2.56824×10^{-26}	1033.58
140	900	9.26443×10^{-47}	4.99958×10^{-36}	3.34507×10^{-26}	2226.04	3.34507×10^{-26}	2226.04

Table 2. DCS of the angle distribution for the Al_{13}^{25} nuclei.

θ	ε	$d\sigma_{0e}$	$d\sigma_{0m}$	$d\sigma_{0q}$	$d\sigma_{0\Omega}$	dE	dM
100	500	9.65125×10^{-43}	3.87337×10^{-34}	2.31052×10^{-26}	6.85932	2.31052×10^{-26}	6.85932
100	700	3.58054×10^{-43}	2.81646×10^{-34}	3.29299×10^{-26}	19.1624	3.29299×10^{-26}	19.1624
100	900	1.70692×10^{-43}	2.21948×10^{-34}	4.28980×10^{-26}	41.2676	4.28980×10^{-26}	41.2676

Continued

120	500	5.16349×10^{-43}	2.94458×10^{-34}	2.25038×10^{-26}	9.4358	2.25038×10^{-26}	9.4358
120	700	1.9156×10^{-43}	2.14111×10^{-34}	3.20729×10^{-26}	26.3617	3.20729×10^{-26}	26.3617
120	900	9.13206×10^{-44}	1.6873×10^{-34}	4.17817×10^{-26}	56.774	4.17817×10^{-26}	56.774
140	500	5.53419×10^{-45}	7.02064×10^{-35}	1.00937×10^{-26}	88.786	1.00937×10^{-26}	88.786
140	700	2.05287×10^{-45}	5.10524×10^{-35}	1.43822×10^{-26}	248.06	1.43822×10^{-26}	248.06
140	900	9.78555×10^{-46}	4.02331×10^{-35}	1.87324×10^{-26}	534.251	1.87324×10^{-26}	534.251

3.2. The Effect of Mass for Be_4^9 and Al_{13}^{25} Nucleus on the Electron-Positron Pair Production Process

Studies the effect of mass for the two nuclei by using Equation (5) and Equation (6) at the value of incident angle $\theta = 100^\circ$ and different values of incident photon energies ε = (500 - 900) MeV. In the DCS for Electric Quadrupole $d\sigma_{oq}$ and Magnetic Octupole $d\sigma_{o\Omega}$.

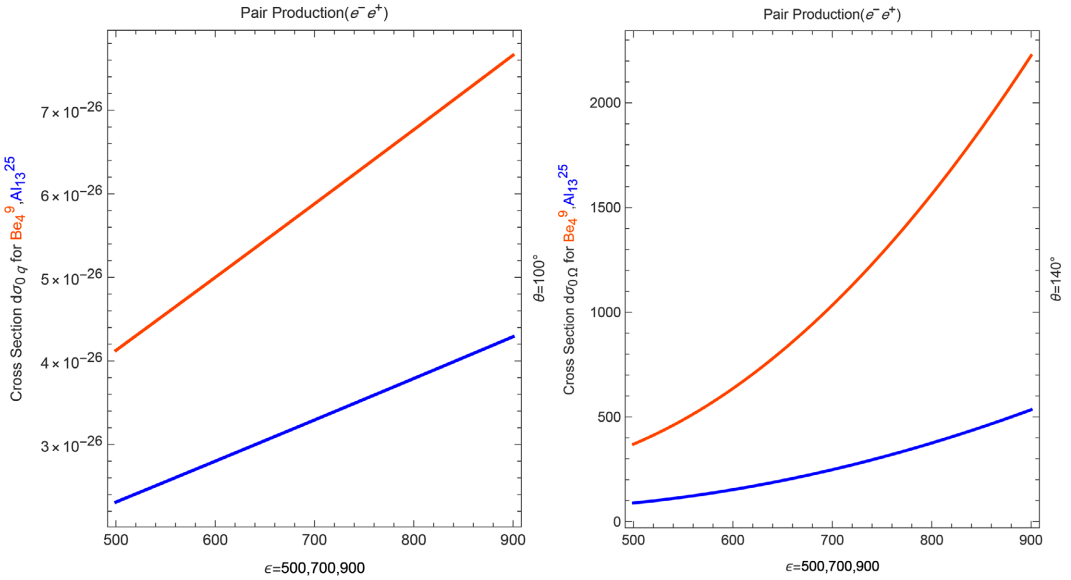

Figure 5. The DCS Electric Quadrupole $d\sigma_{oq}$ and Magnetic Octupole $d\sigma_{o\Omega}$ for the Be_4^9 and Al_{13}^{25} nuclei.

From **Figure 5**, We notice that:

The production rate of the electron-positron pair at the same scattering angles $\theta = 100^\circ$ and different energies increases for both the Electric Quadrupole $d\sigma_{oq}$ and Magnetic Octupole $d\sigma_{o\Omega}$ components when interacting with the light nucleus Be_4^9. The higher production rate observed for the lighter nucleus (Be_4^9) can be attributed to reduced nuclear screening effects and more favorable kinematic conditions. Although the pair production cross section generally scales with Z^2, the effective interaction in lighter nuclei can lead to enhanced emission probabilities under the chosen normalization and multipole contributions.

3.3. The Effect of Electric (*dE*) and Magnetic (*dM*) Fields on the Electron-Positron Pair Production Process for the Be_4^9 and Al_{13}^{25} Nuclei

The impact of electric and magnetic fields on electron-positron pair production, focusing on their relative contribution and determining the most effective interaction for enhancing production rate and modifying pair characteristics. At the value of incident angle $\theta = 100°$ and different values of incident photon energies ε = (500 - 900) MeV.

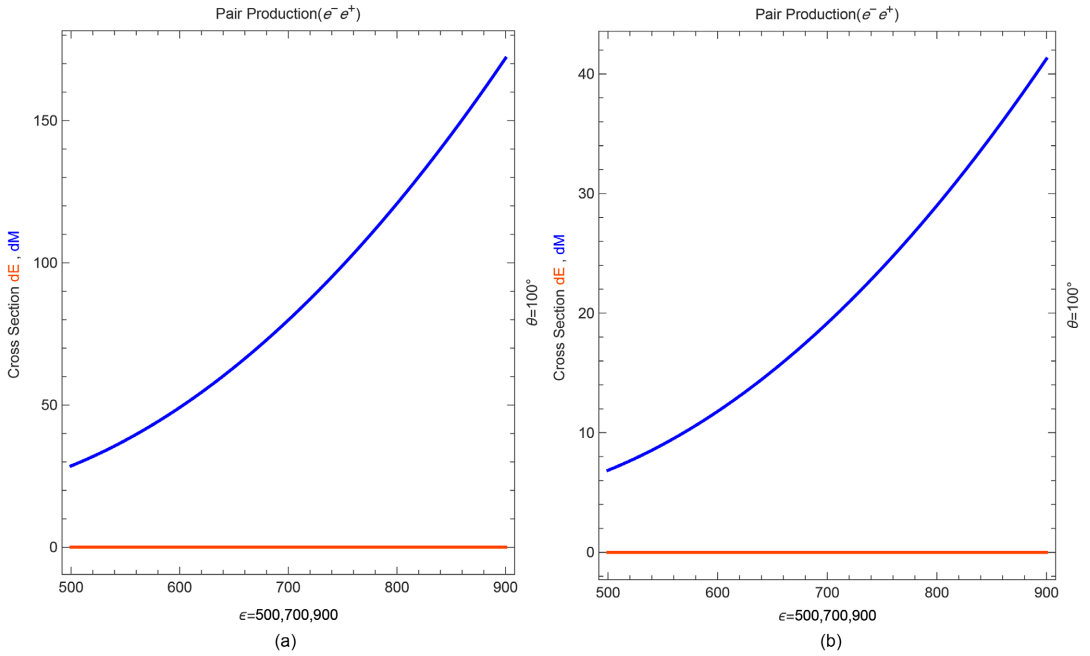

Figure 6. (a) for Be_4^9 nuclei and (b) for and Al_{13}^{25} nuclei. The DCS total Electric field ($dE = d\sigma_{oe} + d\sigma_{oq}$) and DCS total Magnetic field ($dM = d\sigma_{om} + d\sigma_{o\Omega}$).

From **Figure 6**, we can observe that:

- A magnetic field accelerates the electron-positron pair's production rate. For example, the DCS for *dE* of the Be_4^9 nuclei at $\varepsilon = 900$ MeV and $\theta = 100^\circ$ is 7.660356×10^{-26}, but the DCS for dM is 171.948198. Also, for the Al_{13}^{25} nuclei at $\varepsilon = 900$ MeV and $\theta = 100^\circ$, the DCS for *dE* is $4.28979967 \times 10^{-26}$, but the DCS for *dM* is 41.26756772. These findings are consistent with the operating principles of positron emission tomography (PET). It should be noted that both *dE* and *dM* are calculated using the same normalization and units. The observed dominance of the magnetic contribution is therefore a genuine physical effect rather than a numerical artifact, arising from the stronger contribution of higher-order magnetic multipoles in the selected energy range.

4. Conclusion

Our research found that in the Al_{13}^{25} and Be_4^9 nuclei, with electric charge $d\sigma_{oe}$

and magnetic dipole $d\sigma_{om}$, at an angle $\theta = 100^{\circ}$ and an energy of 500 MeV that the formation of $\left(e^{-}e^{+}\right)$ pairs is more efficient. In the electric quadrupole $d\sigma_{oq}$ at an angle $\theta = 100^{\circ}$ and an energy of 900 MeV and in the magnetic dipole $d\sigma_{o\Omega}$ nuclei we have seen that at an angle $\theta = 100^{\circ}$ and an energy of 900 MeV, the formation of $\left(e^{-}e^{+}\right)$ pairs becomes more efficient. The results indicate that lighter nuclei produce $\left(e^{-}e^{+}\right)$ pairs more efficiently. Furthermore, the findings indicate that the magnetic field demonstrates a higher efficiency in facilitating electron-positron pair production in comparison to the electric field. This conclusion is consistent with observations in positron emission tomography (PET) scanners which has been conducted in [14]. Moreover, the results highlighted the strong dependence of pair production efficiency on both the incident photon energy and the angular distribution. These results are consistent with the findings of the [29]-[31].

Data Availability

The data supporting the findings of this study are included within the article.

Conflicts of Interest

The authors declare no conflicts of interest regarding the publication of this paper.

References

[1] Greiner, W. and Reinhardt, J. (2008) Quantum Electrodynamics. Springer.

[2] Griffiths, D. (2020) Introduction to Elementary Particles. John Wiley & Sons.

[3] Zettili, N. (2009) Quantum Mechanics: Concepts and Applications. 2nd Edition, Wiley.

[4] Schwinger, J. (1951) On Gauge Invariance and Vacuum Polarization. *Physical Review*, **82**, 664-679. https://doi.org/10.1103/physrev.82.664

[5] Brezin, E. and Itzykson, C. (1970) Pair Production in Vacuum by an Alternating Field. *Physical Review D*, **2**, 1191-1199. https://doi.org/10.1103/physrevd.2.1191

[6] Marinov, M.S. and Popov, V.S. (1977) Electron-positron Pair Creation from Vacuum Induced by Variable Electric Field. *Fortschritte der Physik*, **25**, 373-400. https://doi.org/10.1002/prop.19770250111

[7] Vinnik, D.V., Alkofer, R., Schmidt, S.M., Smolyansky, S.A., Skokov, V.V. and Prozorkevich, A.V. (2002) Coupled Fermion and Boson Production in a Strong Background Mean Field. *Few-Body Systems*, **32**, 23-39. https://doi.org/10.1007/s00601-002-0110-8

[8] Dumlu, C.K. and Dunne, G.V. (2011) Interference Effects in Schwinger Vacuum Pair Production for Time-Dependent Laser Pulses. *Physical Review D*, **83**, Article ID: 065028. https://doi.org/10.1103/physrevd.83.065028

[9] He, L., Xie, B., Guo, X. and Wang, H. (2012) Electron-positron Pair Production in an Arbitrary Polarized Ultrastrong Laser Field. *Communications in Theoretical Physics*, **58**, 863-871. https://doi.org/10.1088/0253-6102/58/6/13

[10] Blinne, A. and Gies, H. (2014) Pair Production in Rotating Electric Fields. *Physical Review D*, **89**, Article ID: 085001. https://doi.org/10.1103/physrevd.89.085001

[11] Akal, I., Villalba-Chávez, S. and Müller, C. (2014) Electron-Positron Pair Production in a Bifrequent Oscillating Electric Field. *Physical Review D*, **90**, Article ID: 113004.

https://doi.org/10.1103/physrevd.90.113004

[12] Fillion-Gourdeau, F. and MacLean, S. (2015) Time-dependent Pair Creation and the Schwinger Mechanism in Graphene. *Physical Review B*, **92**, Article ID: 035401. https://doi.org/10.1103/physrevb.92.035401

[13] Gies, H. and Klingmüller, K. (2005) Pair Production in Inhomogeneous Fields. *Physical Review D*, **72**, Article ID: 065001. https://doi.org/10.1103/physrevd.72.065001

[14] Dunne, G.V. and Wang, Q. (2006) Multidimensional Worldline Instantons. *Physical Review D*, **74**, Article ID: 065015. https://doi.org/10.1103/physrevd.74.065015

[15] Hebenstreit, F., Alkofer, R. and Gies, H. (2010) Schwinger Pair Production in Space- and Time-Dependent Electric Fields: Relating the Wigner Formalism to Quantum Kinetic Theory. *Physical Review D*, **82**, Article ID: 105026. https://doi.org/10.1103/physrevd.82.105026

[16] Kleinert, H., Ruffini, R. and Xue, S. (2008) Electron-Positron Pair Production in Space- or Time-Dependent Electric Fields. *Physical Review D*, **78**, Article ID: 025011. https://doi.org/10.1103/physrevd.78.025011

[17] Kim, S.P. and Page, D.N. (2007) Improved Approximations for Fermion Pair Production in Inhomogeneous Electric Fields. *Physical Review D*, **75**, Article ID: 045013. https://doi.org/10.1103/physrevd.75.045013

[18] Han, W., Ruffini, R. and Xue, S. (2010) Electron-Positron Pair Oscillation in Spatially Inhomogeneous Electric Fields and Radiation. *Physics Letters B*, **691**, 99-104. https://doi.org/10.1016/j.physletb.2010.06.021

[19] Tarakanov, A.V., Reichel, A.V., Smolyansky, S.A., Schmidt, S.M. and Vinnik, D.V. (2002) Kinetics of Vacuum Pair Creation in Strong Electromagnetic Fields. arXiv: hep-ph/0212200.

[20] Ruf, M., Mocken, G.R., Müller, C., Hatsagortsyan, K.Z. and Keitel, C.H. (2009) Pair Production in Laser Fields Oscillating in Space and Time. *Physical Review Letters*, **102**, Article ID: 080402. https://doi.org/10.1103/physrevlett.102.080402

[21] Tanji, N. (2009) Dynamical View of Pair Creation in Uniform Electric and Magnetic Fields. *Annals of Physics*, **324**, 1691-1736. https://doi.org/10.1016/j.aop.2009.03.012

[22] Sauter, F. (1931) Über das Verhalten eines Elektrons im homogenen elektrischen Feld nach der relativistischen Theorie Diracs. *Zeitschrift für Physik*, **69**, 742-764. https://doi.org/10.1007/bf01339461

[23] Breit, G. and Wheeler, J.A. (1934) Collision of Two Light Quanta. *Physical Review*, **46**, 1087-1091. https://doi.org/10.1103/physrev.46.1087

[24] Bethe, H. and Heitler, W. (1934) On the Stopping of Fast Particles and on the Creation of Positive Electrons. *Proceedings of the Royal Society of London. Series A, Containing Papers of a Mathematical and Physical Character*, **146**, 83-112. https://doi.org/10.1098/rspa.1934.0140

[25] Heisenberg, W. and Euler, H. (1936) Folgerungen aus der Diracschen Theorie des Positrons. *Zeitschrift für Physik*, **98**, 714-732. https://doi.org/10.1007/bf01343663

[26] Hubbell, J.H. (2006) Electron-Positron Pair Production by Photons: A Historical Overview. *Radiation Physics and Chemistry*, **75**, 614-623. https://doi.org/10.1016/j.radphyschem.2005.10.008

[27] Hubbell, J.H. and Seltzer, S.M. (2004) Cross Section Data for Electron-Positron Pair Production by Photons: A Status Report. *Nuclear Instruments and Methods in Physics Research Section B: Beam Interactions with Materials and Atoms*, **213**, 1-9. https://doi.org/10.1016/s0168-583x(03)01524-6

[28] Alkhateeb, S. (2020) Effect of Nuclear Magnetic Distribution on Thephoto Produc-

tion of Longitudinally Polarizedlepton-Pairs in the Field of Na_{11}^{23} and Al_{13}^{27} Nuclei. *Thermal Science*, **24**, 139-147. https://doi.org/10.2298/tsci20s1139a

[29] Alkhateeb, S.A., Alshaery, A.A. and Aldosary, R.A. (2022) Electron-Positron Pair Production in Electro-Magnetic Field. *Journal of Applied Mathematics and Physics*, **10**, 237-244. https://doi.org/10.4236/jamp.2022.102017

[30] Althurwi, Y.O., Alkhateeb, S.A. and Almuallem, N.A. (2025) $e^{-}e^{+}$ Pair Production Using High Energy. *World Journal of Mechanics*, **15**, 105-115. https://doi.org/10.4236/wjm.2025.156006

[31] Abuelhia, E.I. (2006) The Potential Use of Three Photon Positron Annihilation Processes as a New Imaging Modality for Positron Emission Tomography (PET). Ph.D. Thesis, University of Surrey (United Kingdom).

[32] Hawking, S.W. (1974) Black Hole Explosions? *Nature*, **248**, 30-31. https://doi.org/10.1038/248030a0

[33] Fraley, G.S. (1968) Supernovae Explosions Induced by Pair-Production Instability. *Astrophysics and Space Science*, **2**, 96-114. https://doi.org/10.1007/bf00651498

[34] Esnault, L., d'Humières, E., Arefiev, A. and Ribeyre, X. (2021) Electron-Positron Pair Production in the Collision of Real Photon Beams with Wide Energy Distributions. *Plasma Physics and Controlled Fusion*, **63**, Article ID: 125015. https://doi.org/10.1088/1361-6587/ac2e3e